J Mater Sci (2011) 46:7443–7448
DOI 10.1007/s10853-011-5710-6

Synthesis, structure, and properties of the non-centrosymmetric borate $Rb_2CaB_8O_{26}H_{24}$

Jiang Luo · Shilie Pan · Hongyi Li · Zhongxiang Zhou · Zhihua Yang

Received: 31 March 2011 / Accepted: 10 June 2011 / Published online: 21 June 2011

Abstract Single crystals of $Rb_2CaB_8O_{26}H_{24}$, a new non-centrosymmetric borate material, have been grown with sizes up to $8 \times 5 \times 3$ mm^3 by the slow evaporation of water solution at room temperature. The structure of the compound was determined by single-crystal X-ray diffraction. It crystallizes in the orthorhombic system, space group $P2_12_12_1$ with $a = 11.5288(3)$ Å, $b = 12.6334(4)$ Å, $c = 16.6966(4)$ Å, $Z = 4$ and $R_1 = 0.0405$, w$R_2 = 0.1043$. Ultraviolet (UV)–vis spectrum transmission is performed on the $Rb_2CaB_8O_{26}H_{24}$, which shows an absorption edge about 195 nm in the UV region. Thermal properties were investigated by TG–DSC analysis. The powder second-harmonic generation (SHG) intensity measured by the Kurtz-Perry method indicates that $Rb_2CaB_8O_{26}H_{24}$ has about one-third of KDP (KH_2PO_4). The influence of different molar ratios and evaporation speed of water solution on crystal quality and size was also performed on the reported material.

Introduction

In recent years, there has been considerable progress in the development of coherent sources based on nonlinear optical (NLO) crystals [1–7]. Because of their broad transparent region, high damage threshold and moderate birefringence, borate crystals such as β-BaB_2O_4 (BBO), LiB_3O_5 (LBO), and $KBe_2BO_3F_2$ (KBBF) [8–10] are one kind of important NLO material from near-IR to vacuum UV spectral regions [11–22]. The excellent NLO properties of borates are attributed to their various anionic groups, with planar BO_3 and tetrahedral BO_4 groups as basic structures, and this BO_3 triangles and BO_4 tetrahedra can form a variety of compact poly ions by corner sharing of oxygen atoms. Among various anionic groups, the planar BO_3 has attracted our attention, because the highly localized valence electrons, and anisotropy polarizability indicate that some borates are likely to be good candidates for further deep UV NLO materials [23–26]. Though many UV NLO materials have been discovered, these NLO materials have their own drawbacks that limit their applications, for example, it's hard to grow large KBBF crystals because of weak binding between its layered structure units [14]. Therefore, the research of other new NLO materials is still needed. On the basis of detailed analysis on the component elements, rubidium and calcium borates were chosen as the candidate, and the non-centrosymmetric material $Rb_2CaB_8O_{26}H_{24}$ was investigated.

The $Rb_2CaB_8O_{26}H_{24}$ ($Rb_2Ca[B_4O_5(OH)_4]_2{\cdot}8H_2O$) compound was reported in 2003 and its structure has been determined [27]. However, further understanding of the relationship between the structure and the properties of $Rb_2CaB_8O_{26}H_{24}$ prompted us to reinvestigate its crystal structure using the single-crystal X-ray diffraction technique. To the best of our knowledge, the studies focused on the crystal growth and second-order NLO properties of $Rb_2CaB_8O_{26}H_{24}$ have not been reported in the literature. In this article, we present the crystal growth, optical properties, and the relationship between the structure and the properties of the $Rb_2CaB_8O_{26}H_{24}$ crystal.

J. Luo · S. Pan (✉) · H. Li · Z. Zhou · Z. Yang
Xinjiang Key Laboratory of Electronic Information Materials and Devices, Xinjiang Technical Institute of Physics & Chemistry, Chinese Academy of Sciences, 40-1 South Beijing Road, Urumqi 830011, China
e-mail: slpan@ms.xjb.ac.cn

J. Luo · H. Li
Graduate School of the Chinese Academy of Sciences, Beijing 100039, China

Table 1 Crystal data and structure refinement for RbCBOH

Empirical formula	$Rb_2CaB_8O_{26}H_{24}$
Temperature	296(2) K
Wavelength	0.71073 Å
Formula weight	737.69
Crystal system	Orthorhombic
Space group	$P2_12_12_1$
Unit cell dimensions	$a = 11.5288(3)$ Å
	$b = 12.6334(4)$ Å
	$c = 16.6966(4)$ Å
Volume	2431.83(12) $Å^3$
Z	4
Density (calculated)	2.015 g/cm^3
Absorption coefficient	4.343/mm^{-1}
F(000)	1464
Crystal size	0.34 × 0.30 × 0.25 mm^3
Theta range for data collection	2.02–25°
Index ranges	$-12 \le h \le 13$, $-15 \le k \le 12$, $-19 \le l \le 19$
Reflections collected	9691
Independent reflections	4211 [R(int) = 0.0270]
Completeness to theta = 25	99.3%
Refinement method	Full-matrix least-squares on F^2
Goodness-of-fit on F^2	1.073
Final R indices [$I > 2\sigma(I)$][a]	$R_1 = 0.0405$, $wR_2 = 0.1043$
R indices (all data)[a]	$R_1 = 0.0466$, $wR_2 = 0.1075$
Largest diff. peak and hole	2.105 and −1.013 e $Å^{-3}$

[a] $R_1 = \Sigma||F_o^2|-|F_c||/\Sigma|F_o^2|$ and $wR_2 = [\Sigma w(F_o^2-F_c^2)^2/\Sigma w F_o^{24}]^{1/2}$ for $F_o^2 > 2\sigma(F_o^2)$

Experimental section

Single-crystal growth

Single crystals of $Rb_2CaB_8O_{26}H_{24}$ (RCBOH) were synthesized through slow evaporation. Rb_2CO_3, $CaCl_2$, and H_3BO_3 powders were mixed in a molar ratio of 2:1:8. In this experiment, 11.547 g of Rb_2CO_3 (Jiangxin Lithium Factory, 90%) and 12.366 g of H_3BO_3 (Beijing Chemical Co., Ltd., 99.5%) were dissolved in approximately 100 mL deionized water first, after CO_2 release, the above solution was mixed with 2.750 g $CaCl_2$ (Tianjin Baishi Chemical Industry Co., Ltd., 99.5%) to form a flocculent precipitate which was amorphous when studied by powder XRD. The mixture was stirred during 15 min at 80 °C and leaving at room temperature. After 4 weeks, the single crystals were obtained. Crystals were rated qualitatively as low or high based on whether light scattering from a He–Ne laser could be observed by eye.

Powder X-ray diffraction

Powder XRD was performed on an automated Bruker D8 ADVANCE X-ray diffractometer equipped with a diffracted-beamed monochromatic set for Cu Kα (λ = 1.5418 Å) radiation and a nickel filter at room temperature in the angular range from 10 to 70° (2θ) with a scanning step width of 0.02° and a fixed counting time of 1 s/step.

X-ray crystallographic studies

A colorless and transparent crystal of RCBOH with dimensions 0.34 × 0.30 × 0.25 mm^3 was chosen for structure determination. Single-crystal X-ray intensity date were collected at 296 K on a SMART APEX II diffractometer using monochromatized Mo Kα radiation ($\lambda = 0.71073$ Å). The crystal structure was solved by the direct method and refined in SHELXTL crystallographic software package by full-matrix least-squares methods on F_o^2. The structures were checked for missing symmetry elements with PLATON [28]. Crystal data and structure refinement information are summarized in Table 1.

Infrared spectroscopy

IR spectrum of the ground crystals in the range of 400–4000 cm^{-1} was recorded on a BRUKER EQUINOX 55 Fourier transform infrared spectrometer using samples prepared as KBr pellets.

Table 2 The influence of different molar ratios to the crystal growth

Sample number	The molar ratio of Rb_2CO_3:$CaCl_2$:H_3BO_3	The result	Excessive element	Growth rate	Crystal quality
1	1:1:8	No crystal	–	–	–
2	2:1:8	RCBOH	Rb	Moderate	High
3	1:1:4	RCBOH	Rb, Ca	High	Low
4	0.5:1:4	RBOH	Ca	Moderate	High
5	0.5:1:8	RBOH + H_3BO_3	Ca, B	High	Low
6	1:1:12	RBOH + H_3BO_3	B	High	Low
7	2:1:12	RCBOH + H_3BO_3	Rb, B	High	Low

Thermal analysis

The TG–DSC analysis were carried out on a simultaneous Netzsch STA 449C thermal analyzer instrument, with a heating rate of 10 °C min^{-1} in an atmosphere of flowing N_2 from 25 to 1100 °C.

UV–vis transmission spectroscopy

UV–vis transmission spectrum data for RCBOH crystal sample was collected with a TU-1901UV–Vis–NIR spectrophotometer at room temperature, which can operate over the range 190–900 nm.

Powder SHG measurements

A preliminary SHG efficiency measurement of RCBOH has been carried out by the Kurtz-Perry method using microcrystalline samples at room temperature [29]. Micro crystalline KDP served as the standard. About 90 mg of powder was pressed into a pellet, which was then irradiated with a pulsed IR beam (10 ns and 10 kHz) produced by a Q-switched Nd:YAG laser of wavelength 1064 nm. A 532 nm filter was used to absorb the fundamental and pass the visible light onto a photomultiplier. A combination of a half-wave achromatic retarder and a polarizer was used to control the intensity of the incident power, which was measured with an identical photomultiplier connected to the same high-voltage source. The SHG efficiency has been shown to depend strongly on particle size; thus the RCBOH crystal were ground and sieved into distinct particle size ranges [29]. To make relevant comparisons with known SHG materials, we also ground and sieved crystalline KDP into the same particle size ranges.

Results and discussion

Synthesis and growth

In the process of RCBOH crystal growth, the influence of different molar ratios and evaporation speed of water solution on crystal quality and size has been studied. When the initial reagents and reaction ratio were changed, another compound, $Rb[B_5O_6(OH)_4]\cdot 2H_2O$ (RBOH) [30] was obtained. In our study the compound of RBOH was very easy obtained. The RCBOH crystal could not be obtained when the initial reagents mixed in a stoichiometric ratio (Rb_2CO_3:$CaCl_2$:H_3BO_3 = 1:1:8). In Table 2, it can be seen that the molar ratio of Rb_2CO_3 is the critical influential factor to acquire RCBOH crystals. By comparing the samples 2, 3, and 7, it was further confirmed that only when the Rb_2CO_3 exceeds, RCBOH crystal with high quality can be obtained. The ratio of 2:1:8 (Rb_2CO_3:$CaCl_2$:H_3BO_3) is chosen as the proper molar ratio in this experiment. Fast growth speed leads to the formation of crystals with poor optical quality and slow speed spends too much time. In this experiment the crystals were obtained from the amorphous precipitate, and crystallized completely after 4 weeks. The fluctuation of growth temperature is also a bad factor for the crystal quality.

The obtained crystals are colorless. As shown in Fig. 1, the maximum size is about 8 × 5 × 3 mm^3. The typical XRD pattern of RCBOH is shown in Fig. 2. The experimental powder XRD pattern of RCBOH is in agreement with the calculated one based on the single-crystal data, suggesting that the synthesized phase is pure.

Crystal structure

Single crystal X-ray diffraction data were obtained. The refinement of 419 parameters with 4211 observed reflections [$I \geqq 2\sigma$] resulted in the residuals of R_1/wR_2 = 0.0405/0.1043. The RCBOH structure consists of $[B_4O_5(OH)_4]^{2-}$ polyborate anions, Ca^{2+} and Rb^+ cations, and H_2O molecules. According to the classification of polyborate anions proposed by Burns, Grice, and Hawthorne [31, 32], the fundamental building blocks (FBBs) shorthand notation for $[B_4O_5(OH)_4]^{2-}$ in RCBOH is 2Δ2□: <Δ2□>=<Δ2□>, the symbol gives the number of BO_3 triangles(Δ) and BO_4 tetrahedra(□) in the form $m\Delta n\square$, where m and n are integers representing the number of BO_3 and BO_4 (Fig. 3).

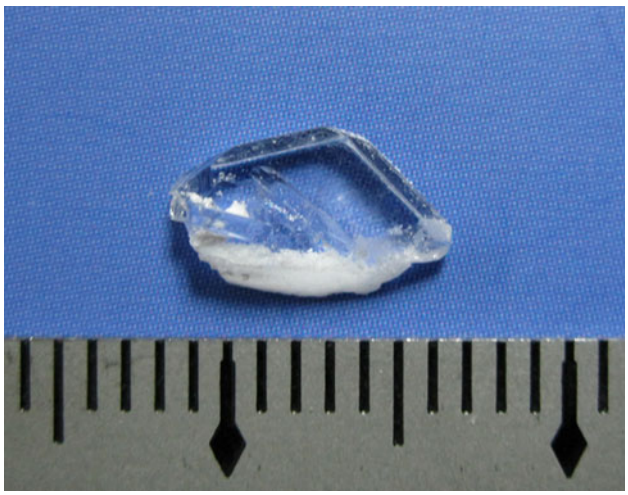

Fig. 1 Photograph of RCBOH crystal (The minimum scale of the ruler is one millimeter)

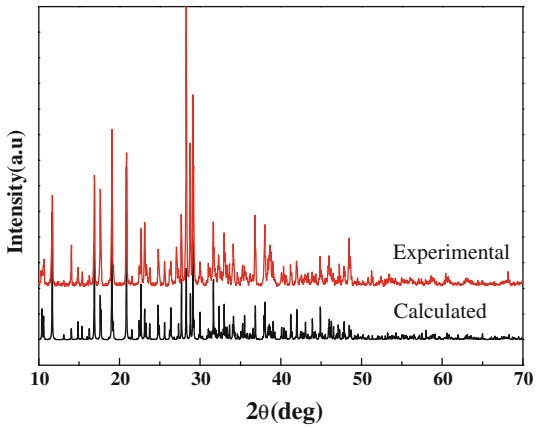

Fig. 2 XRD pattern of RCBOH crystal

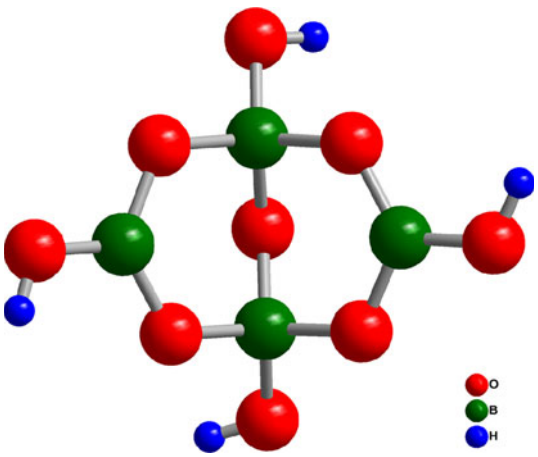

Fig. 3 Structural unit $[B_4O_5(OH)_4]^{2-}$ in RCBOH

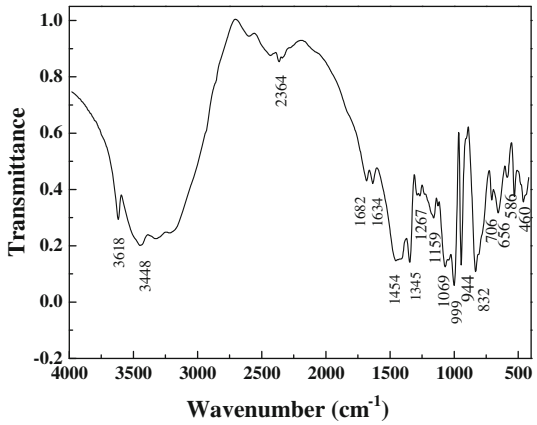

Fig. 4 IR spectrum of RCBOH crystal

Infrared spectroscopy

Seen from Fig. 4, the characteristic peaks of the RCBOH crystal can be described as follows: The peak at 460 cm^{-1} can be attributed to the bending of BO_4 [33]. Peaks at 706, 656, 586 cm^{-1} can be assigned as the bending mode of BO_3 groups. Peaks at 1345 and 944 cm^{-1} can be asymmetric and symmetric stretching vibration of BO_3. Strong peaks at 999 and 832 cm^{-1} can be assigned as asymmetric and symmetric stretching vibration of BO_4, respectively. The weak bands at 1268–1159 cm^{-1} can be attributed to in-plane bending mode of B–O–H. Peaks at 1682 and 1634 cm^{-1} can be assigned as H–O–H bending mode. Peaks between 3000 and 3600 cm^{-1} can be attributed to the stretching vibrations of OH group and the water molecules which are involved in the hydrogen bonding.

TG–DSC analysis

The thermal behavior of RCBOH is shown in Fig. 5. TG analysis curve shows that a weight loss of about 29.5% from 70 to 1050 °C, which corresponds to the loss of eight crystal water molecules and eight hydroxyl groups (Theoretical water loss: 29.3%). In the DSC curve, the first endothermic peak appearing at 124.5 °C is related to the dehydration of RCBOH. The endothermic peak appearing at 638.6 °C is related to the melting of the solid phase.

UV–vis transmission spectroscopy

The transmission spectrum for RCBOH is shown in Fig. 6, it can be seen that a wide transmission range is observed with the UV absorption edge about 195 nm. The observed maximum transmittance rate of RCBOH crystal is up to 70%, although the thickness of the measured crystal sample is about 3 mm.

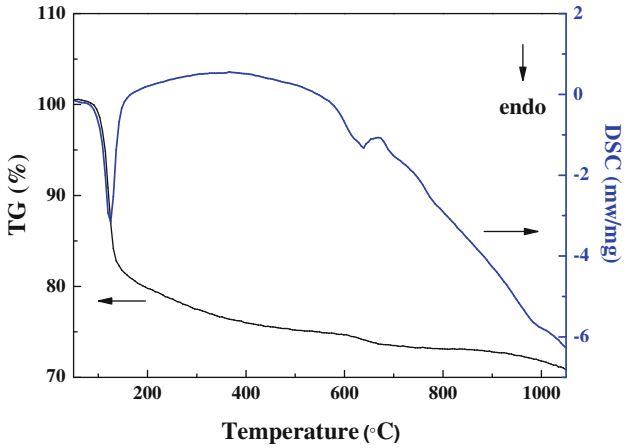

Fig. 5 TG–DSC curves of RCBOH

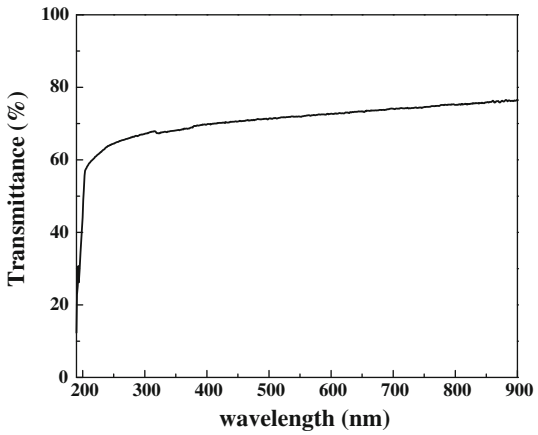

Fig. 6 Optical transmission spectrum for RCBOH crystal

NLO measurements

On the basic of non-centrosymmetric RCBOH crystal structure, it is expected to possess NLO properties. According to the anionic group theory of NLO activity in borates [34], the BO_3 trigonal planes are responsible for the large SHG effects, and the BO_4 groups contribute less. The orientation of these groups also determines their total NLO contribution. The arrangement of $[B_4O_5(OH)_4]^{2-}$ groups in RCBOH is in an unfavorable manner so that the overall SHG efficiency of RCBOH is about one-third of KDP. The powder SHG profile of the RCBOH compound is shown in Fig. 7, demonstrating that the SHG signal increases gradually with increasing particle size. Furthermore, moderate green-light output was observed when 1064 nm-laser permeated the crystal along a special direction. All of these show that the RCBOH compound is phase matchable.

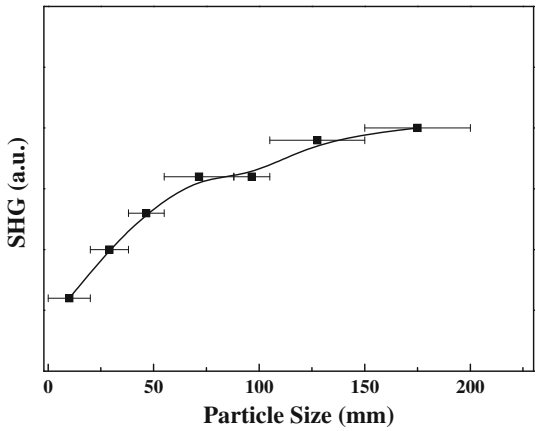

Fig. 7 Phase-matching curve, i.e., particle size versus SHG intensity, for RCBOH. The *solid curve* drawn is to guide the eye and is not a fit to the data

Conclusions

In summary, good-quality, and fairly large-sized RCBOH crystals with non-centrosymmetric structure has been prepared by aqueous solutions. It exhibits the SHG efficiency is about one-third of KDP. Our studies indicate that by the introduction of the rubidium and calcium into the borate system, we can design new types of second order NLO materials. Our future research efforts will be devoted to the exploration of new SHG compounds by introduction of other type of alkali metal or alkali earth metal into the borates.

Acknowledgements This study is supported by the Main Direction Program of Knowledge Innovation of Chinese Academy of Sciences (Grant KJCX2-EW-H03-03), National Natural Science Foundation of China (Grant 50802110, 21001114), One Hundred Talents Project Foundation Program of Chinese Academy of Sciences, Western Light Joint Scholar Foundation Program of Chinese Academy of Sciences.

References

1. Becker P (1998) Adv Mater 10:979
2. Sasaki T, Mori Y, Yoshimura M, Yap Y, Kamimura T (2000) Mater Sci Eng R 30:1
3. Ye N, Stone-sundberg JL, Hruschka MA, Aka G, Kong W, Keszler DA (2005) Chem Mater 17:2687
4. Kong F, Jiang HL, Hu T, Mao JG (2008) Inorg Chem 47:10611
5. Penin N, Seguin L, Gerand B, Touboul M, Nowogrocki G (2002) J Alloys Compd 334:97
6. Dhanuskodi S, Philominal A, Philip J, Kim K, Yi J (2011) J Mater Sci 46:3169. doi:10.1007/s10853-010-5200-2
7. Reshak AH, Auluck S et al (2006) J Mater Sci 41:1927. doi:10.1007/s10853-006-4487-5
8. Chen CT, Wu BC, Jiang AD, You GM (1985) Sci Sin B 18:235
9. Chen CT, Wu YC, Jiang A, You G, Li R, Lin S (1989) J Opt Soc Am B6:616
10. Wang GL, Zhou Y, Li CM, Xu ZY, Wang XY, Zhu Y, Chen CT (2008) Appl Phys B91:95

11. Becker P, Liebertz J, Bohaty L (1999) J Cryst Growth 203:149
12. Mao JG, Jiang HL, Fang K (2008) Inorg Chem 47:8498
13. Pan SL, Wu YC, Fu PZ, Zhang GC, Li ZH, Du CX, Chen CT (2003) Chem Mater 15:2218
14. Chen CT, Wang YB, Wu BC, Wu KC, Zeng WL, Yu LH (1995) Nature 373:322
15. Yuan X, Shen DZ, Wang XQ, Shen GQ (2006) J Cryst Growth 292:458
16. Wu YC, Sasaki T, Nakai S, Yokotani A, Tang HG, Chen CT (1993) Appl Phys Lett 62:2614
17. Liu YS, Dentz D, Belt R (1983) Opt Lett 9:76
18. Kato KJ (1986) IEEE J Quantum Electron 31:169
19. Barbier J, Penin N, Cranswick LM (2005) Chem Mater 17:3130
20. Zyss J, Oudar JL (1982) Phys Rev A 26:2028
21. Halasyamani PS, O'Hare D (1998) Chem Mater 10:646
22. Hagerman ME, Poeppelmeier KR (1995) Chem Mater 7(4):602
23. Leonyuk NIJ (1997) J Cryst Growth 174:301
24. Marder SR, Beratan DN, Cheng LT (1991) Science 252:103
25. Touboul M, Penin N, Nowogrocki G (2009) Solid State Sci 5:1327
26. Muller EA, Cannon RJ, Sarjeant AN, Ok KM, Halasyamani PS, Norquist A (2005) Cryst Growth Des 5:1913
27. Zhu LX, Yue T, Gao SY, Hu MC, Yu KB (2003) J Mol Struct 658:215
28. Spek AL (2003) J Appl Crystallogr 36:7
29. Kurtz SQ, Perry TT (1968) J Appl Phys 39:3798
30. Behm H (1984) Acta Crystallogr C40:217
31. Burns PC, Grice JD, Hawthorne FC (1995) Can Mineral 33:1131
32. Grice JD, Burns PC, Hawthorne FC (1999) Can Mineral 37:731
33. Li J, Xia SP, Gao SY (1995) Spectrochim Acta 51:519
34. Chen CT, Liu GZ (1986) Annu Rev Mater Sci 16:203